Brain Reactivity to Smoking Cues Prior to Smoking Cessation Predicts Ability to Maintain Tobacco Abstinence

Amy C. Janes, Diego A. Pizzagalli, Sarah Richardt, Blaise deB. Frederick, Sarah Chuzi, Gladys Pachas, Melissa A. Culhane, Avram J. Holmes, Maurizio Fava, A. Eden Evins, and Marc J. Kaufman

Background: Developing the means to identify smokers at high risk for relapse could advance relapse prevention therapy. We hypothesized that functional magnetic resonance imaging (fMRI) reactivity to smoking-related cues, measured before a quit attempt, could identify smokers with heightened relapse vulnerability.

Methods: Before quitting smoking, 21 nicotine-dependent women underwent fMRI during which smoking-related and neutral images were shown. These smokers also were tested for possible attentional biases to smoking-related words using a computerized emotional Stroop (ES) task previously found to predict relapse. Smokers then made a quit attempt and were grouped based on outcomes (abstinence vs. slip: smoking $\geq$ 1 cigarette after attaining abstinence). Prequit fMRI and ES measurements in these groups were compared.

Results: Slip subjects had heightened fMRI reactivity to smoking-related images in brain regions implicated in emotion, interoceptive awareness, and motor planning and execution. Insula and dorsal anterior cingulate cortex (dACC) reactivity induced by smoking images correlated with an attentional bias to smoking-related words. A discriminant analysis of ES and fMRI data predicted outcomes with 79% accuracy. Additionally, smokers who slipped had decreased fMRI functional connectivity between an insula-containing network and brain regions involved in cognitive control, including the dACC and dorsal lateral prefrontal cortex, possibly reflecting reduced top-down control of cue-induced emotions.

Conclusions: These findings suggest that the insula and dACC are important substrates of smoking relapse vulnerability. The data also suggest that relapse-vulnerable smokers can be identified before quit attempts, which could enable personalized treatment, improve tobacco-dependence treatment outcomes, and reduce smoking-related morbidity and mortality.

Key Words: Dorsal anterior cingulate cortex, emotional Stroop task, fMRI, insula , relapse, smoking cessation, tobacco

Tobacco-related illness is estimated to cause more than 5 million yearly deaths in the developed world (1). By 2030, the yearly smoking-related death toll is expected to rise to 8 million unless current smoking trends are reversed (1). Although most smokers would like to quit (2) and nicotine dependence treatments exist (3–5), relapse rates remain high (6–8). Because relapse vulnerability is strongly influenced by smoking-cue reactivity (9), developing a better understanding of neurobiological mechanisms underlying smoking-cue reactivity may lead to new treatments. From a clinical perspective, developing the means to identify relapse-vulnerable smokers before smoking cessation would allow for personalized treatment, possibly reducing smoking relapse and associated morbidity and mortality.

Functional MRI (fMRI) may be useful to identify brain regions and circuits underlying relapse vulnerability. Functional MRI studies of smokers have reported various brain areas that are reactive to smoking-related cues (10–12). However, it is unknown whether fMRI reactivity to smoking cues can predict relapse vulnerability. Therefore, we determined whether fMRI smoking-cue reactivity before a smoking cessation attempt relates to smoking outcomes by assessing smoking-cue brain reactivity in smokers about to quit smoking. The clinical outcome of interest by which smoking-cue-reactivity data were grouped was smoking any part of a cigarette after attaining at least 24 hours of abstinence (a "slip"). Slips occur early in the course of smoking cessation attempts, are triggered by exposure to smoking-related cues (13), and are highly predictive of relapse in naturalistic (8,14–17) and controlled (18) studies. It was hypothesized that fMRI reactivity to smoking-related cues would differ based on short-term cessation outcomes.

We investigated whether slip subjects exhibited different group-level whole-brain fMRI activation patterns. To develop a neuroanatomic model predictive of individual smoking cessation outcomes, individual subject data were used to examine the effects of smoking-related cues on specific brain regions including the insula, dorsal anterior cingulate (dACC), dorsolateral prefrontal cortex (DLPFC), and amygdala. The insula was a main focus because it is reactive to smoking-related cues (19), may mediate cue-induced craving (20), and is thought to be critical for maintaining tobacco dependence (21). The anterior insula may be particularly important because it is hypothesized to be the site of interoceptive awareness and is active during a range of subjective feeling states (22). The ACC was targeted because it is anatomically connected to the insula (22), both regions coactivate in studies of interoceptive awareness, and the dACC activates when smokers attempt to resist cue-induced craving (10), possibly reflecting an effort to exert cognitive control (23). Functional MRI reactivity in the left DLPFC was assessed because high-frequency transcranial magnetic stimulation over the left DLPFC reduces cigarette craving and consumption (24). The

Brain Imaging Center (ACJ, SR, BdeBF, MJK) McLean Hospital, Harvard Medical School, Belmont; Department of Psychology (DAP, AJH), Harvard University, Cambridge; and Massachusetts General Hospital (SC, GP, MAC, MF, AEE), Harvard Medical School, Boston, Massachusetts.

Authors AEE and MJK contributed equally to this work.

Address correspondence to Amy C. Janes, Ph.D., Brain Imaging Center, McLean Hospital, 115 Mill Street, Belmont, MA 02478; E-mail: ajanes@mclean.harvard.edu.

Received Sep 22, 2009; revised Dec 29, 2009; accepted Dec 30, 2009.

0006-3223/10/$36.00
doi:10.1016/j.biopsych.2009.12.034

amygdala was also investigated because it plays a role in initial responses to emotionally salient stimuli (25), including smoking cues (11). Because interactions between brain regions may be important in regulating smoking cue reactivity (26), a functional connectivity analysis was conducted on the same fMRI data. We evaluated whether functional connectivity of a network containing the anterior insula and dACC differed as a function of the ability to maintain abstinence.

Behavioral performance on an emotional Stroop (ES) task, which has been shown to identify recently abstinent smokers with heightened relapse vulnerability (27), was assessed. It is unknown whether an attentional bias for smoking-related words, measured with the ES before smoking cessation, can predict relapse vulnerability.

It was hypothesized that, before quitting, smokers who would slip would have greater fMRI reactivity to smoking-related images and disrupted functional connectivity of the insula/dACC network. We also hypothesized that an attentional bias for smoking-related words on the ES task would correlate with fMRI reactivity to smoking-related images in the insula, dACC, left DLPFC, and amygdala, and these measures would predict smoking cessation outcomes.

Methods and Materials

Subjects

Twenty-one women underwent neuroimaging at McLean Hospital before participating in a smoking cessation clinical trial at Massachusetts General Hospital (MGH; NCT00218465). Subjects met DSM-IV criteria for current nicotine dependence, reported smoking ≥10 cigarettes per day in the previous 6 months, and had expired air carbon monoxide (CO) >10 ppmv at screening. Smokers with current unstable medical illness, pregnancy, recent drug and alcohol use (QuickTox 11 Panel Drug Test Card, Branan Medical, Irvine, California; Alco-Sensor IV, Intoximeters, St. Louis, Missouri), major depressive disorder, alcohol use disorder in the prior 6 months, current psychotropic drug use, or lifetime diagnosis of organic mental or psychotic disorders were excluded. Only women were enrolled because the parent clinical trial involved an investigational medication not approved for use in men. The Institutional Review Boards at MGH and McLean Hospital approved this study. Subjects provided written informed consent and were compensated for participation.

Baseline smoking behavior was characterized by recording and measuring pack-years of tobacco smoking, expiratory CO levels (Bedfont Micro IV Smokerlyzer, Bedfont Scientific, Kent, England), the number of cigarettes smoked the morning before imaging, and by administering the Fagerstrom Test for Nicotine Dependence (FTND) (28). Group differences (slip vs. abstinence) were assessed with two-sided Student's *t* tests.

Emotional Stroop Task

Nineteen subjects performed a computerized ES task (27) before smoking cessation in which smoking-related and neutral words, matched for length and use frequency in the English language, were displayed in red, green, or blue fonts, using Eprime software (Psychology Software Tools, Pittsburgh, Pennsylvania). Subjects were instructed to report (by button press) word color as quickly and accurately as possible and to ignore word meaning. After a 96-trial practice block of letter strings, four 33-trial experimental blocks separated by 5-sec breaks were run in the following word order: neutral, smoking, smoking, neutral. To replicate prior studies and avoid smoking-related word carryover effects, analyses were restricted to the first two blocks (as per Waters *et al.* [27], Heatherton *et al.* [29], and McKenna [30]). Analyses considering all four blocks yielded similar findings (see Results).

Each trial began with a fixation cross (500 msec), followed by word presentation until a response was made, followed by a 500-msec intertrial interval. If no response occurred within 3 sec, the word disappeared, and a new trial started after 500 msec. A 500-msec tone was presented after incorrect or absent responses. Reaction times (RT) and accuracies were recorded by computer.

To minimize outlier response effects, outlier trials (150 msec < RT < 1500 msec) were excluded, as were trials with natural log-transformed RT falling outside the range of mean ± 3 SD. Mixed analyses of covariance (ANCOVAs) were run separately on accuracy and RT scores entering Group (slip, abstinent) as between-subject factors, Condition (neutral vs. smoking-related words) as repeated measures and FTND scores as covariates (subjects who eventually slipped had higher baseline FTND scores; see Results). Group × Condition interactions indicated significant group differences in ES task interference effects, computed as $\text{Accuracy}_{\text{Neutral}} - \text{Accuracy}_{\text{Smoking}}$ and $\text{RT}_{\text{Smoking}} - \text{RT}_{\text{Neutral}}$. Higher RT/accuracy values indicated smoking-related interference effects.

Neuroimaging

Smoking was not restricted until shortly before imaging. During fMRI, subjects viewed smoking-related (people smoking, hands holding cigarettes, or cigarettes alone) or neutral (general content-matched but no smoking cues) images (11,31). Animal images were shown to prompt subjects to press a response button and were included to ensure subjects attended to stimuli but were not used in data analyses. Forty-two smoking-related, 40 neutral, and 8 animal images were presented in 6 equal-length blocks. Each image was presented pseudo-randomly for 4 sec with no more than two of the same stimulus type appearing consecutively. A fixation cross appeared for 14 sec between images.

Scans were acquired on a Siemens Trio 3 Tesla scanner (Erlangen, Germany) with a circularly polarized head coil. Multiplanar rapidly acquired gradient-echo structural images (repetition time [TR] = 2.1 sec, echo time [TE] = 2.7 msec, slices = 128, matrix = 256 × 256, flip angle = 12°, resolution = 1.0 × 1.0 × 1.33 mm) and gradient echo echo-planar images (TR = 2 sec, TE = 30 msec, matrix = 64 × 64 mm, field of view = 224, flip angle = 75°, slices = 30, resolution = 3.5 mm isotropic with 0 mm gap) were acquired.

fMRI Analyses

Images were analyzed using Brain Voyager QX 1.10.4 (Brain Innovation, Maastricht, the Netherlands). Images were slice-time corrected, motion corrected, spatially smoothed (6-mm Gaussian kernel), resampled to 3 × 3 × 3 mm isotropic voxels, and spatially normalized into Talairach space. To reduce motion-related variability, a program (based on Lemieux *et al.* [32]) was used to model out time points (1.2% of all data points) exhibiting motion >1.75 mm (half voxel size).

A whole-brain fixed-effects general linear model (GLM) was run using image regressors (smoking, neutral, animal images) and motion confound regressors. The 2-gamma hemodynamic response function was convolved with square waves defined by the onset–offset of each image presentation. Beta maps comparing smoking with neutral images were created for each subject.

These maps were used to compare fMRI activity between slip and abstinent subject groups using a random-effects analysis.

Multiple comparisons were cluster-level corrected (33). To determine the cluster extent necessary to correct for multiple comparisons, a Monte Carlo simulation (a standard method used to correct multiple comparisons) (34), was run with MATLAB script Cluster-threshold-beta (35). In a single simulation, the minimum size of each contiguous voxel cluster was determined by modeling the functional image matrix (64 × 64 × 30 voxels), by assuming an individual voxel Type 1 error of $p = .01$, and by smoothing the activation map by a three-dimensional 6-mm full width at half maximum Gaussian kernel. Following 10,000 simulations, the cluster size probability was determined and the cluster extent that yielded $p = .005$ (31 three-mm resampled isotropic voxels, ~837 mm^3) was selected, which is more conservative than accepted threshold levels (36).

Region-of-Interest (ROI) Analyses: Relation to Smoking Cessation Outcome and Emotional Stroop Performance

Beta weights for the smoking image > neutral image contrasts were extracted from the anterior insula, dACC, DLPFC, and amygdala, using the Brain Voyager ROI analysis tool. Beta weights were averaged across all voxels within each ROI. The insula and amygdala ROIs were defined anatomically, and the DLPFC and dACC were defined on the basis of the functional connectivity analysis (Figure S1 in Supplement 1). A Pearson's correlation coefficient was calculated to evaluate possible relationships between ROI fMRI activation and ES task performance. To determine whether prequit fMRI and ES findings could discriminate slip from abstinent subjects, a discriminant analysis using a cross-validation approach was performed. The cross-validation used a leave-one-out classification strategy, in which each case was iteratively classified on the basis of all other cases, to minimize the possible effects of single subjects on the discriminant function.

Independent Component Analysis (ICA)

The ICA was performed on cue-reactivity fMRI data to determine functional connectivity between insula and frontocingulate areas. ICA was chosen rather than a seed-region-based approach because ICA more effectively removes artifacts stemming from functional connectivity analyses based on seed regions (37). Additionally, ICA is superior for separating independent functional networks, allowing the selection of a network containing the bilateral insula, the anterior cingulate, and other frontal brain structures from other networks in which the insula may be involved.

The Group ICA fMRI Toolbox v1.3e (GIFT) (38) was used to identify the independent component containing the bilateral insula and ACC. Because group ICA requires that all data be analyzed simultaneously, a principal-component analysis data reduction step was run to load all data into memory. Data then were concatenated into a matrix, and a group spatial ICA was performed using the infomax algorithm. ICA splits fMRI data into independent components, which are temporally correlated groupings of fMRI signals that represent independent functional networks. The GIFT minimum description length algorithm determined that 25 optimal components existed. All 25 maps representing average connectivity for all 21 subjects were visually inspected. On the basis of our a priori hypothesis, Component Number 2 containing bilateral insula and anterior cingulate (but not spurious connectivity signal in white matter or ventricles) was selected for further analysis.

Next, each participant's Component Number 2 time course was converted into a Brain Voyager–compatible regressor, and a random effects GLM was run containing the Component Number 2 time course and motion confound regressors. The Component Number 2 activation map for all 21 subjects was Bonferroni corrected to $p < .01$ and compared between slip and abstinence subjects, using a random effects analysis. Multiple comparisons were corrected to $p \leq .005$ with the Monte Carlo procedure described earlier.

Smoking Cessation

After prequit imaging and other assessments, all subjects quit smoking during the 8-week smoking cessation phase of the clinical trial. Interventions included a weekly, manualized individual behavioral intervention, nicotine patch (21 mg/day for 4 weeks, 14 mg/day for 2 weeks, 7 mg/day for 2 weeks), and 2-mg nicotine polacrilex gum or lozenge, up to 12 mg/day, to be used as needed. All participants quit smoking for at least 24 hours. Following 24 hours abstinence, participants who smoked any cigarettes during the nicotine replacement therapy (NRT) treatment period were considered at high risk for relapse (slip group), and those who did not smoke during this period were considered at low relapse risk (abstinence group). Our criteria were based on a Society for Research on Nicotine and Tobacco's working group definition of relapse as smoking seven or more consecutive days or more than once/week for two or more consecutive weeks, and a slip as smoking any amount less than this following at least 24 hours abstinence (39). Smoking status was established by weekly self-report of smoking behavior in the prior 7 days using the Timeline Followback Method (40,41) and weekly expired CO measurements. Subjects who self-reported abstinence and had an expired CO <9 ppmv were considered abstinent.

Results

Of the 21 subjects who completed prequit neuroimaging, nine slipped while on NRT. Slips took place on average 17.4 days (range: 1–49 days) after established abstinence. Slip and abstinence groups differed at a trend level on FTND scores ($t_{19} = 2.0$, $p < .07$; Table 1) and not on any other demographic variable. Of the 19 subjects completing the ES task, eight slipped, and these groups differed on FTND scores ($t_{17} = 2.12$, $p < .05$). In the entire clinical trial cohort ($n = 126$) from which study subjects were recruited, slips were strong predictors of relapse (odds ratio = 4.25, 95% confidence interval: 1.41–12.79, $p < .01$).

Functional MRI Results

Whole-Brain Analysis. A whole-brain mixed-effects analysis revealed that, relative to the abstinent group, the slip group had greater smoking-related versus neutral image reactivity in the bilateral insula, ACC, posterior cingulate cortex, amygdala, primary motor cortex, premotor cortex, inferior parietal cortex, parahippocampal gyrus, thalamus, putamen, cerebellar hemispheres and vermis, prefrontal cortex, and striate and extrastriate cortex ($t_{19} = 2.86$, cluster corrected $p \leq .005$, Figure 1, Table S1 in Supplement 1).

Emotional Stroop Task. A mixed group (slip, abstinence) × condition (neutral vs. smoking-related words) ANCOVA, adjusting for FTND scores, was conducted. For both reaction time [$F(1,16) = 7.30$, $p < .02$] and accuracy [$F(1,16) = 7.98$, $p < .015$], the group × condition was significant, due to significantly higher smoking-related interference effects ($RT_{Smoking} - RT_{Neutral}$ and $Accuracy_{Neutral} - Accuracy_{Smoking}$) in slip subjects ($n = 8$)

Table 1. Demographic Information and Emotional Stroop Data

Group	Eventual slip Subjects (n = 9)	Abstinence Subjects (n = 12)
Age (years)	47.7 ± 8.6	44.4 ± 12.3
Carbon Monoxide (ppmv)	19.2 ± 9.2	21.4 ± 8.2
Cigarettes Smoked Prior to Scan	4.4 ± 2.1	4.3 ± 2.0
FTND	6.8 ± 1.4	5.1 ± 2.3[a]
Ham-D	3.6 ± 3.3	1.2 ± 1.7
Pack-Years	33.0 ± 24.8	25.8 ± 17.2
Days on NRT	46.9 ± 20.9	48.7 ± 11.8
Emotional Stroop Interference Effect (accuracy: % correct)	.016 ± .030[c]	.020 ± .019[b,d]
Emotional Stroop Interference Effect (reaction time; msec)	71.03 ± 59.67[c]	−.14 ± 58.06[b,d]

Age, carbon monoxide levels, and cigarettes smoked before scan were measured on the day of functional magnetic resonance imaging (fMRI scan). Cigarettes smoked before scan refers to the number of cigarettes subjects smoked on the fMRI scan day. FTND, Ham-D (54), and pack-years were assessed at screening before the fMRI scan day. Days on NRT are the total number of days subjects were treated with NRT during their quit attempt. Emotional Stroop $accuracy_{neutral} - accuracy_{smoking}$ represents the difference in response accuracy for neutral minus smoking words. $RT_{Smoking} - RT_{Neutral}$ represents the difference in reaction time for responding to neutral minus smoking words. Two neuroimaging participants (one in each group) did not perform the emotional Stroop task. Data are represented as mean ± SD.

FTND, Fagerstrom Test for Nicotine Dependence; Ham-D, Hamilton Depression Rating Scale; NRT, nicotine replacement therapy.

[a] Groups differ at a trend level at $p < .07$.

[b] Groups differ at $p < .01$.

[c] $n = 8$.

[d] $n = 11$.

relative to abstinent subjects (n = 11; Table 1). Highlighting the specificity of these findings, there was no main effect of group either for accuracy [$F(1,16) = .303$, $p > .59$] or reaction time [$F(1,16) = .04$, $p > .84$]. Group × Condition effects were replicated for the reaction time measure when considering all four blocks [reaction time: $F(1,16) = 4.56$, $p < .05$; and accuracy: $F(1,16) = 1.52$, $p > .23$].

Correlations Between FMRI and Emotional Stroop Data

Right and left anterior insula fMRI reactivity was strongly correlated ($r = .93$, $p < .001$); accordingly, the mean bilateral anterior insula activity was used for correlation analyses. In subjects undergoing both fMRI and the ES task (n = 19), mean anterior insula ROI beta weights were significantly correlated with task interference effects (accuracy: $r = -.62$, $p < .006$; RT: $r = .51$, $p < .03$), as were the beta weights for the dACC (accuracy: $r = -.53$, $p < .025$; RT: $r = .41$, $p < .083$). For the left DLPFC and amygdala, no correlations emerged (all $p > .11$). Thus, participants with the strongest anterior insula and dACC fMRI activation to smoking-related images showed the largest interference effects. Hierarchical regression analyses confirmed that ES interference effects predicted mean insular and dACC activity after controlling for FTND scores [mean insula, accuracy: $\Delta R^2 = .38$, $\Delta F(1,16) = 9.98$, $p < .007$; RT: $\Delta R^2 = .25$, $\Delta F_{1,16} = 5.36$, $p < .04$; dACC, accuracy: $\Delta R^2 = .39$, $\Delta F(1,16) = 11.20$, $p < .005$].

Given group differences in ES effects and insula/dACC activation, a discriminant analysis was conducted to determine whether prequit data could discriminate slip from abstinent subjects. Stroop interference RT (Wilks's $\lambda = .71$) and accuracy effects (Wilks's $\lambda = .60$) as well as mean anterior insula fMRI reactivity (Wilks's $\lambda = .73$) were all significant outcome predictors [all Fs$(1,17) > 6.21$, ps $< .025$], whereas dACC fMRI reactivity was not (Wilks's $\lambda = .95$). Further, when all four predictors were included, the overall model was significant [$\chi^2(4) = 10.44$, $p < .035$] and correctly classified 5 of 8 slip and 10 of 11 abstinent subjects (78.9% correct classification rate). A model including only the ES interference effects and the mean insula reactivity was also significant [$\chi^2(3) = 9.23$, $p < .026$] and correctly classified 73.7% of cross-validated grouped cases (8 of 11 abstinent and 6 of 8 slip subjects).

Functional Connectivity Results

In light of our a priori hypothesis concerning the insula and the ACC (22), a network containing the insula and ACC was identified from the ICA functional connectivity analysis. This network included temporal and frontal cortical regions, the rostral and dACC, surrounding frontal regions (including pre- and primary motor cortex and prefrontal cortex), and primary and association visual areas within the occipital and parietal cortex. The network also included the thalamus, amygdala, caudate nucleus, putamen, brainstem, and cerebellar hemispheres ($t_{20} = 7.80$, Bonferroni corrected $p \leq .01$, Figure 2; Table S2 in Supplement 1). When comparing this network between subjects who slipped and maintained abstinence, slip subjects showed decreased functional connectivity between this network and the left insula, adjacent inferior frontal gyri, prefrontal cortex, ACC, primary and premotor cortex, primary somatosensory cortex, cerebellum, superior and middle temporal gyrus, putamen, and primary visual and visual association cortices ($t_{20} = 2.85$, cluster corrected $p \leq .005$, Figure 2; Table S3 in Supplement 1).

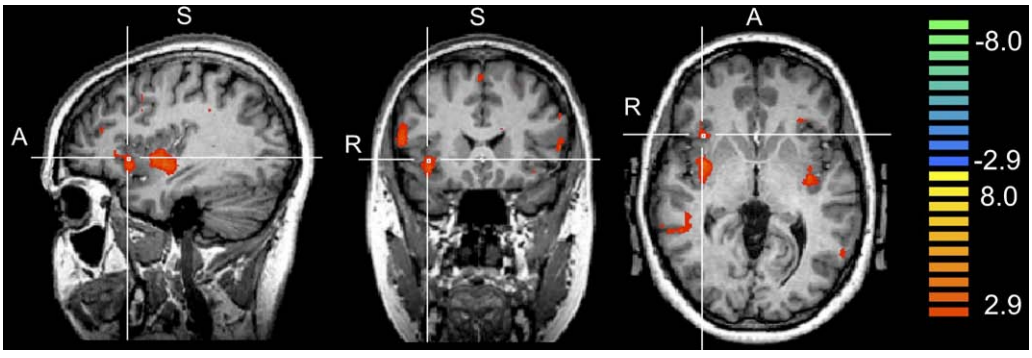

Figure 1. Whole-brain analysis of prequit brain reactivity to smoking-related versus neutral images compared between subjects who did and did not slip. Subjects who slipped exhibited greater functional magnetic resonance imaging reactivity in several brain areas (Table S1 in Supplement 1), including the right anterior insula [$t_{19} = 2.86$, cluster corrected, $p \leq .005$]. Talairach (55) coordinates: $x = 35$, $y = 18$, $z = 0$. A, anterior; S, superior; R, right.

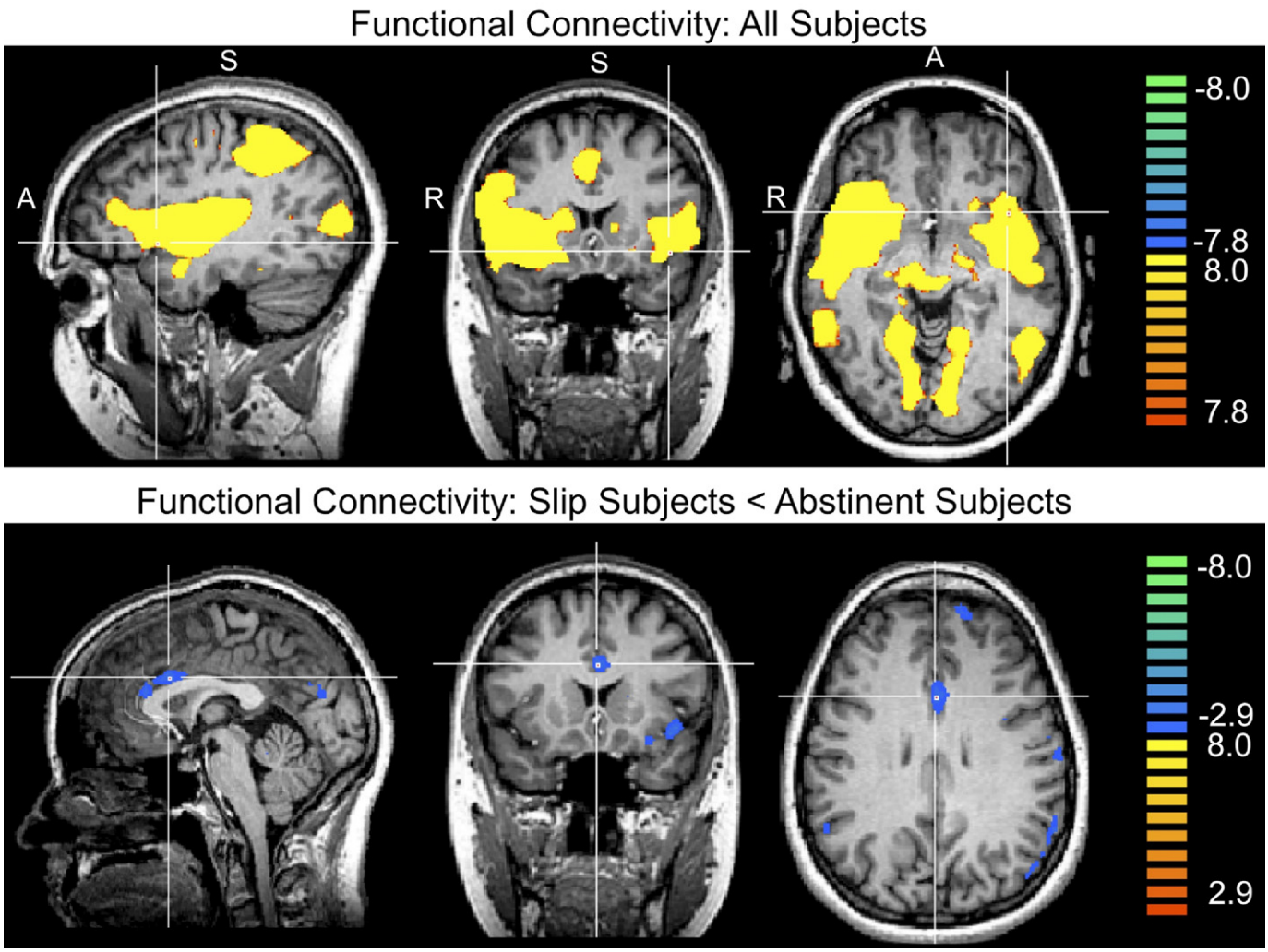

Figure 2. Functional connectivity analyses. Top: the prequit network was identified in 21 subjects and contained bilateral insula and anterior cingulate cortex. Crosshairs are positioned in the anterior insula; Talairach (55) coordinates: $x = -38$, $y = 13$, $z = -6$, $t(20) = 7.80$, Bonferroni corrected $p = .01$ (Table S2 in Supplement 1). Bottom: prequit network connectivity differences between slip ($n = 9$) versus abstinence ($n = 12$) subjects were found in the dorsal anterior cingulate and other brain areas (Table S3 in Supplement 1). Talairach (55) coordinates for the dorsal anterior cingulate cortex: $x = 0$, $y = 13$, $z = 26$, $t_{20} = 2.85$, cluster corrected, $p \leq .005$). A, anterior; R, right; S, superior.

Discussion

Smokers who slipped during the quit attempt exhibited increased prequit brain fMRI reactivity to smoking-related images in the insula, amygdala, and several other brain areas. Insula and amygdala activation might imply that smoking-related images are more emotionally salient and may induce interoceptive awareness to a greater extent than neutral images in smokers vulnerable to relapse. Our insula findings are in line with evidence suggesting that this region is involved in maintaining smoking behavior and processing smoking- and other drug-related cues (19,21). Slip subjects also had increased reactivity to smoking-related images in motor control and planning areas such as ACC, prefrontal cortex, and others involved in motor behavior (e.g., premotor cortex, cerebellum) (42), replicating data indicating that smoking cues enhance brain reactivity in regions related to tool use (43). This enhanced reactivity raises the possibility that, in the presence of smoking-related stimuli, vulnerable subjects may be more likely to prepare for or initiate motor responses geared toward reducing interoceptive sensations related to craving.

Functional Connectivity Findings

The functional connectivity analysis identified a network including the insula and ACC, which are structurally connected and coactivate in studies of interoceptive awareness (22). This network included brain regions involved in emotional processing (e.g., amygdala, insula) (25) and in reactivity to smoking-related cues (amygdala, thalamus, cuneus, insula) (11,12,44). Slip subjects had reduced prequit connectivity between this network and brain regions involved in response inhibition (45), such as the dACC and DLPFC. Slip subjects also had less connectivity between the overall network and the left insula, an interesting finding because the left insula may bridge communications between the executive-control and interoceptive networks (46). The connectivity findings along with impaired ES performance suggest that slip subjects may have decreased top-down control of emotion regulation. This could result in increased interocep-

tive awareness of smoking-related cues, leading to enhanced smoking cue-reactivity, ES interference effects, and relapse vulnerability.

Correlation Analyses

The mean bilateral insula fMRI activation to smoking-related images was correlated with indexes of increased attentional bias to smoking-related words, possibly reflecting a behavioral phenotype of relapse vulnerability (27). This correlation may result from the insula's role in interoceptive awareness (22). Attention to internal states such as craving on exposure to smoking cues and words could increase attentional bias toward smoking-related words and thus be associated with increased interference scores on the ES task. These findings suggest that the insula is an important brain substrate of relapse vulnerability. Additionally, dACC activation was found to correlate with decreased accuracy to name the color of smoking-related words. Dorsal ACC activation increases when smokers try to resist cue-induced craving (10), which may reflect greater effort to maintain cognitive control over craving responses (47). We found decreased functional connectivity between the dACC and insula, suggesting that the ability of the dACC to regulate insula and interoceptive states may be disrupted in subjects who will eventually slip. One interpretation is that slip subjects, with reduced dACC functional connectivity, may exhibit greater dACC activity in response to smoking-related cues as an attempt to maintain top-down control of interoceptive and emotional states.

We conclude that increased smoking-related anterior insula and dACC reactivity and ES attentional bias may reflect potentiated relapse vulnerability. Consistent with this assumption, a discriminant analysis including mean bilateral insula and dACC fMRI reactivity and ES interference effects predicted, with high accuracy, which smokers would slip after attaining initial smoking abstinence. Our model remained predictive after controlling for nicotine dependence severity, using the FTND. The FTND may account for some but not likely all residual variance, suggesting that other aspects of dependence-related variance including plasma nicotine and cotinine levels may have contributed to group differences. The ability of fMRI and ES to predict short-term outcomes warrants confirmation in an independent sample to determine whether these measurements have utility as a clinical prediction tool. Such a tool could be used to personalize treatment and enrich clinical trials of novel smoking relapse prevention treatments with subjects more likely to relapse, potentially reducing variability and accelerating drug discovery.

Limitations

An important caveat is that this study only included women. Because smoking-cue-reactivity and craving differ by sex (44,48), it is unclear whether our findings generalize to men. However, no sex differences were reported for the effects of insular lesions on smoking behavior (21), and no sex differences in insula reactivity to smoking cues have been reported (44), suggesting that sex differences minimally influence study findings. In addition, menstrual cycle phase was not controlled for, and we cannot rule out a possible influence of menstrual cycle on the findings. One argument against this possibility is that participants underwent fMRI and the ES task, and quit smoking, over different time intervals that span menstrual cycle phases (8.2 ± 4.7 days apart), with no difference between slip and abstinence groups. Thus, we believe our findings, and in particular the correlation between anterior insula fMRI smoking cue reactivity and ES interference effects, are not attributable to menstrual cycle effects. We intend to examine the effects of sex and menstrual cycle phase in future fMRI cue reactivity studies.

Future Directions

Follow-up studies are needed to validate our observation that fMRI and ES can predict short-term cessation outcomes. Such information should help prospectively identify smokers who would benefit from standard therapies (e.g., NRT) as well as those who may benefit from tailored relapse-prevention treatments, including treatments that may modulate insula reactivity to smoking-related cues. For example, the macaque insula is enriched in corticotrophin-releasing factor 1 (CRF-1) receptors (49), and in rodent work, a CRF-1 receptor antagonist reduced deficits in brain reward function induced by nicotine withdrawal and stress-induced relapse (50). Thus, CRF-1 antagonists may be a useful therapy for smokers with heightened insula reactivity to smoking-related cues. As another example, infusion of the hypocretin-1 receptor-selective antagonist (SB-334687) into the insula of rodents reduced nicotine self-administration (51), and systemically reduced motivation for nicotine and other positive reinforcers (52). Thus, hypocretin receptor antagonists may represent another pharmacologic approach to modulate insula reactivity to smoking-related cues (53) in relapse-vulnerable smokers. We plan to use fMRI to study how different pharmacologic treatments modulate insula smoking cue reactivity and how such effects relate to relapse vulnerability.

Conclusions

We conclude that prequit brain reactivity to smoking-related images is greater in smokers who eventually slip after attaining brief abstinence with NRT and that anterior insula and dACC fMRI cue reactivity correlate with an attentional bias to smoking-related words. The functional connectivity findings suggest that slip subjects had reduced prequit top-down control over interoceptive awareness and may have been less able to regulate emotional responding to smoking-related images. Although these findings pertain directly to smokers, the roles played by the insula in interoceptive awareness (22) and dACC in cognitive control (47) suggest that insula, dACC, and ES assessments may be useful to identify vulnerable individuals with other disorders influenced by incentive-related cues, including other addictive disorders.

This research was supported in part by National Institute on Drug Abuse Grant Nos. U01DA019378, R01DA022276, R01DA014674, R01DA09448, K02DA017324, and T32DA015036; by funding from the Counter-Drug Technology Assessment Center (CTAC), an office within the Office of National Drug Control Policy (ONDCP) via Army Contracting Agency Contract BK39-03-C-0075; and by research support from GlaxoSmithKline. We thank Dr. David Schoenfeld (Massachusetts General Hospital) for his contributions to this study. We thank Drs. Robert S. Ross, Bruce M. Cohen, and Elizabeth Quattrocki-Knight for comments on the original manuscript.

The following authors reported no biomedical financial interests or potential conflicts of interest. ACJ, BBF, SR, SC, GP, MC, AH. DAP has received research support from GlaxoSmithKline and ANT North America, Inc. (Advanced Neuro Technology), consulting fees from ANT North America, Inc. (Advanced Neuro Technology) and AstraZeneca for projects unrelated to the current study, and honoraria from AstraZeneca. AEE has received research product support from Pfizer and speaker honoraria from Reed Medical Education. MF has received research

support from Abbott Laboratories, Alkermes, Aspect Medical Systems, AstraZeneca, Bio Research, BrainCells, Inc., Bristol-Myers Squibb Company, Cephalon, Clinical Trial Solutions, Eli Lilly and Company, Forest Pharmaceuticals, Inc., Ganeden, GlaxoSmithKline (GSK), J and J Pharmaceuticals, Lichtwer Pharma, GmbH, Lorex Pharmaceuticals, National Alliance for Research on Schizophrenia and Depression, National Center for Complementary and Alternative Medicine, National Institute on Drug Abuse, National Institute of Mental Health, Novartis, Organon, Inc., PamLab, LLC, Pfizer, Inc., Pharmavite, Roche, Sanofi-Aventis, Sbire, Solvay Pharmaceuticals, Inc., Synthelabo, Wyeth-Ayerst Laboratories. MF has performed advisory and consulting for Abbott Laboratories, Amarin, Aspect Medical Systems, AstraZeneca, Auspex Pharmaceuticals, Bayer AG, Best Practice Project Management, Inc, BioMarin Pharmaceuticals, Inc., Biovail Pharmaceuticals, Inc., BrainCells, Inc., Bristol-Myers Squibb Company, Cephalon, Clinical Trials Solutions, CNS Response, Compellis, Cypress Pharmaceuticals, Dov Pharmaceuticals, EISAI, Inc., Eli Lilly and Company, EPIX Pharmaceuticals, Euthymics Bioscience, Inc., Fabre-Kramer, Pharmaceuticals, Inc., Forest Pharmaceuticals, Inc., GSK, Grunenthal, GmbH Janssen Pharmaceutica, Jazz Pharmaceuticals, J and J Pharmaceuticals, Knoll Pharmaceutical Company, Labopharm, Lorex Pharmaceuticals, Lundbeck, MedAvante, Inc., Merck, Methylation Sciences, Neuronetics, Novartis, Nutrition 21, Organon, Inc., PamLab, LLC, Pfizer, Inc., PharmaStar, Pharmavite, Precision Human Biolaboratory, PsychoGenics, Psylin Neurosciences, Inc., Ridge Diagnostics, Inc., Roche, Sanofi-Aventis, Sepracor, Schering-Plough, Solvay Pharmaceuticals, Inc., Somaxon, Somerset Pharmaceuticals, Synthelabo, Takeda, Tetragenex, Trancept Pharmaceuticals, TransForm Pharmaceuticals, Vanda Pharmaceuticals, Inc., Wyeth-Ayerst Laboratories. MF has had speaking/publishing engagements with Adamed Co., Advanced Meeting Partners, American Psychiatric Association, American Society of Clinical Psychopharmacology, AstraZeneca, Belvoir, Boehringer-Ingelheim, Bristol-Myers Squibb Company, Cephalon, Eli Lilly and Company, Forest Pharmaceuticals, Inc., GlaxoSmithKline, Imedex, Novartis, Organon, Inc., Pfizer, Inc., PharmaStar, Massachusetts General Hospital (MGH) Psychiatry Academy/Primedia, MGH Psychiatry Academy/Reed-Elsevier, United BioSource Corporation, Wyeth-Ayerst Laboratories. MF has equity holdings in Compellis and royalty/patent, other income as follows: patent applications for Sequential Parallel Comparison Design and for a combination of azapirones and bupropion in MDD, copyright royalties for the MGH Cognitive and Physical Functioning Questionnaire, Sexual Function Inventory, Antidepressant Treatment Response Questionnaire, Discontinuation Emergent Signs and Symptoms, and SAFER Criteria Inventory. MJK has received research support from GSK, Organon, Varian, Inc., BioPAL, has done advisory/consulting for Amgen, and Novartis.

Supplementary material cited in this article is available online.

1. WHO (2008): *World Health Organization report on the global tobacco epidemic*. The MPOWER package. Available at: http://whqlibdoc.who.int/publications/2008/9789241596282_eng.pdf. Accessed November 2009.
2. Tingen MS, Andrews JO, Gruber JL, Harper RJ (1999): Implementing the Agency for Health Care Policy and Research smoking cessation guidelines: A call to action. *Clin Excell Nurse Pract* 3:323–328.
3. Cahill K, Stead LF, Lancaster T (2008): Nicotine receptor partial agonists for smoking cessation. *Cochrane Database Syst Rev* CD006103.
4. Hughes JR, Stead LF, Lancaster T (2007): Antidepressants for smoking cessation. *Cochrane Database Syst Rev* CD000031.
5. Stead LF, Perera R, Bullen C, Mant D, Lancaster T (2008): Nicotine replacement therapy for smoking cessation. *Cochrane Database Syst Rev* CD000146.
6. Etter JF, Stapleton JA (2006): Nicotine replacement therapy for long-term smoking cessation: A meta-analysis. *Tob Control* 15:280–285.
7. Fiore MC, Smith SS, Jorenby DE, Baker TB (1994): The effectiveness of the nicotine patch for smoking cessation. A meta-analysis. *JAMA* 271:1940–1947.
8. Garvey AJ, Bliss RE, Hitchcock JL, Heinold JW, Rosner B (1992): Predictors of smoking relapse among self-quitters: A report from the normative aging study. *Addict Behav* 17:367–377.
9. Ferguson SG, Shiffman S (2009): The relevance and treatment of cue-induced cravings in tobacco dependence. *J Subst Abus Treat* 36:235–243.
10. Brody AL, Mandelkern MA, Olmstead RE, Jou J, Tiongson E, Allen V, *et al.* (2007): Neural substrates of resisting craving during cigarette cue exposure. *Biol Psychiatry* 62:642–651.
11. Due DL, Huettel SA, Hall WG, Rubin DC (2002): Activation in mesolimbic and visuospatial neural circuits elicited by smoking cues: Evidence from functional magnetic resonance imaging. *Am J Psychiatry* 159:954–960.
12. Franklin TR, Wang Z, Wang J, Sciortino N, Harper D, Li Y, *et al.* (2007): Limbic activation to cigarette smoking cues independent of nicotine withdrawal: A perfusion fMRI study. *Neuropsychopharmacology* 32:2301–2309.
13. Wileyto P, Patterson F, Niaura R, Epstein L, Brown R, Audrain-McGovern J, *et al.* (2004): Do small lapses predict relapse to smoking behavior under bupropion treatment? *Nicotine Tob Res* 6:357–366.
14. Brandon TH, Tiffany ST, Obremski KM, Baker TB (1990): Postcessation cigarette use: The process of relapse. *Addict Behav* 15:105–114.
15. Kenford SL, Fiore MC, Jorenby DE, Smith SS, Wetter D, Baker TB (1994): Predicting smoking cessation. Who will quit with and without the nicotine patch. *JAMA* 271:589–594.
16. Nides MA, Rakos RF, Gonzales D, Murray RP, Tashkin DP, Bjornson-Benson WM, *et al.* (1995): Predictors of initial smoking cessation and relapse through the first 2 years of the lung health study. *J Consult Clin Psychol* 63:60–69.
17. Shiffman S, Paty JA, Gnys M, Kassel JA, Hickcox M (1996): First lapses to smoking: Within-subjects analysis of real-time reports. *J Consult Clin Psychol* 64:366–379.
18. Chornock WM, Stitzer ML, Gross J, Leischow S (1992): Experimental model of smoking re-exposure: Effects on relapse. *Psychopharmacology* 108:495–500.
19. Naqvi NH, Bechara A (2009): The hidden island of addiction: The insula. *Trends Neurosci* 32:56–67.
20. Gray MA, Critchley HD (2007): Interoceptive basis to craving. *Neuron* 54:183–186.
21. Naqvi NH, Rudrauf D, Damasio H, Bechara A (2007): Damage to the insula disrupts addiction to cigarette smoking. *Science* 315:531–534.
22. Craig AD (2009): How do you feel—now? The anterior insula and human awareness. *Nat Rev Neurosci* 10:59–70.
23. Paus T, Koski L, Caramanos Z, Westbury C (1998): Regional differences in the effects of task difficulty and motor output on blood flow response in the human anterior cingulate cortex: A review of 107 PET activation studies. *Neuroreport* 9:R37–R47.
24. Amiaz R, Levy D, Vainiger D, Grunhaus L, Zangen A (2009): Repeated high-frequency transcranial magnetic stimulation over the dorsolateral prefrontal cortex reduces cigarette craving and consumption. *Addiction* 104:653–660.
25. Phillips ML, Drevets WC, Rauch SL, Lane R (2003): Neurobiology of emotion perception I: The neural basis of normal emotion perception. *Biol Psychiatry* 54:504–514.
26. Zhang X, Chen X, Yu Y, Sun D, Ma N, He S, *et al.* (2009): Masked smoking-related images modulate brain activity in smokers. *Hum Brain Mapp* 30:896–907.
27. Waters AJ, Shiffman S, Sayette MA, Paty JA, Gwaltney CJ, Balabanis MH (2003): Attentional bias predicts outcome in smoking cessation. *Health Psychol* 22:378–387.
28. Heatherton TF, Kozlowski LT, Frecker RC, Fagerstrom KO (1991): The Fagerstrom Test For Nicotine Dependence: A revision of the Fagerstrom Tolerance Questionnaire. *Br J Addict* 86:1119–1127.
29. McKenna FP (1986): Effects of unattended emotional stimuli on color-naming performance. *Curr Psychol Res Rev* 5:3–9.

30. Rohsenow DJ, Niaura RS (1999): Reflections on the state of cue-reactivity theories and research [see comment]. *Addiction* 94:343–344.
31. Gilbert DG, Rabinovich NE (1999): International smoking image series (with neutral counterparts), version 1.2. Carbondale, IL: Integrative Neuroscience Laboratory, Department of Psychology, Southern Illinois University.
32. Lemieux L, Salek-Haddadi A, Lund TE, Laufs H, Carmichael D (2007): Modelling large motion events in fMRI studies of patients with epilepsy. *Magn Reson Imaging* 25:894–901.
33. Chumbley JR, Friston KJ (2009): False discovery rate revisited: FDR and topological inference using Gaussian random fields. *Neuroimage* 44: 62–70.
34. Haskins AL, Yonelinas AP, Quamme JR, Ranganath C (2008): Perirhinal cortex supports encoding and familiarity-based recognition of novel associations. *Neuron* 59:554–560.
35. Slotnick SD, Moo LR, Segal JB, Hart J Jr (2003): Distinct prefrontal cortex activity associated with item memory and source memory for visual shapes. *Brain Res Cogn Brain Res* 17:75–82.
36. Ross RS, Slotnick SD (2008): The hippocampus is preferentially associated with memory for spatial context. *J Cogn Neurosci* 20:432–446.
37. Birn RM, Murphy K, Bandettini PA (2008): The effect of respiration variations on independent component analysis results of resting state functional connectivity. *Hum Brain Mapp* 29:740–750.
38. Calhoun VD, Adali T, Pearlson GD, Pekar JJ (2001): A method for making group inferences from functional MRI data using independent component analysis. *Hum Brain Mapp* 14:140–151.
39. Hughes JR, Shiffman S, Callas P, Zhang J (2003): A meta-analysis of the efficacy of over-the-counter nicotine replacement. *Tob Control* 12: 21–27.
40. Sobell LC, Sobell MB (1992): Timeline Followback: A technique for assessing self-reported ethanol consumption. In: Allen J, Litten RZ, editors. *Measuring Alcohol Consumption: Psychosocial and Biological Methods*. Totowa, NJ: Humana Press, 41–72.
41. Sobell LC, Sobell MB (2003): Alcohol consumption measures. In: Allen JP, Wilson VB, eds. *Assessing Alcohol Problems: A Guide for Clinicians and Researchers*, *2nd ed*. Bethesda, MD: NIH/National Institute on Alcohol Abuse and Alcoholism, 75–99.
42. Gerardin E, Sirigu A, Lehericy S, Poline JB, Gaymard B, Marsault C, *et al.* (2000): Partially overlapping neural networks for real and imagined hand movements. *Cereb Cortex* 10:1093–1104.
43. Yalachkov Y, Kaiser J, Naumer MJ (2009): Brain regions related to tool use and action knowledge reflect nicotine dependence. *J Neurosci* 29: 4922–4929.
44. McClernon FJ, Kozink RV, Rose JE (2008): Individual differences in nicotine dependence, withdrawal symptoms, and sex predict transient fMRI-BOLD responses to smoking cues. *Neuropsychopharmacology* 33: 2148–2157.
45. Menon V, Adleman NE, White CD, Glover GH, Reiss AL (2001): Error-related brain activation during a Go/Nogo response inhibition task. *Hum Brain Mapp* 12:131–143.
46. Seeley WW, Menon V, Schatzberg AF, Keller J, Glover GH, Kenna H, *et al.* (2007): Dissociable intrinsic connectivity networks for salience processing and executive control. *J Neurosci* 27:2349–2356.
47. Kerns JG, Cohen JD, MacDonald AW 3rd, Cho RY, Stenger VA, Carter CS (2004): Anterior cingulate conflict monitoring and adjustments in control. *Science* 303:1023–1026.
48. Field M, Duka T (2004): Cue reactivity in smokers: The effects of perceived cigarette availability and gender. *Pharmacol Biochem Behav* 78: 647–652.
49. Mar-Sanchez M, Young LJ, Plotsky PM, Insel TR (1999): Autoradiographic and in situ hybridization localization of corticotropin-releasing factor 1 and 2 receptors in nonhuman primate brain. *J Comp Neurol* 408:365–377.
50. Bruijnzeel AW, Prado M, Isaac S (2009): Corticotropin-releasing factor-1 receptor activation mediates nicotine withdrawal-induced deficit in brain reward function and stress-induced relapse. *Biol Psychiatry* 66: 110–117.
51. Hollander JA, Lu Q, Cameron MD, Kamenecka TM, Kenny PJ (2008): Insular hypocretin transmission regulates nicotine reward. *Proc Natl Acad Sci U S A* 105:19480–19485.
52. Borgland SL, Chang SJ, Bowers MS, Thompson JL, Vittoz N, Floresco SB, *et al.* (2009): Orexin A/hypocretin-1 selectively promotes motivation for positive reinforcers. *J Neurosci* 29:11215–11225.
53. Corrigall WA (2009): Hypocretin mechanisms in nicotine addiction: Evidence and speculation. *Psychopharmacology* 206:23–37.
54. Hamilton M (1967): Development of a rating scale for primary depressive illness. *Br J Soc Clin Psychol* 6:278–296.
55. Talairach J, Tournoux P (1988): *Co-Planar Stereotaxic Atlas of the Human Brain: 3-Dimensional Proportional System: An Approach to Cerebral Imaging*. New York: Thieme Medical.

Supplemental Information

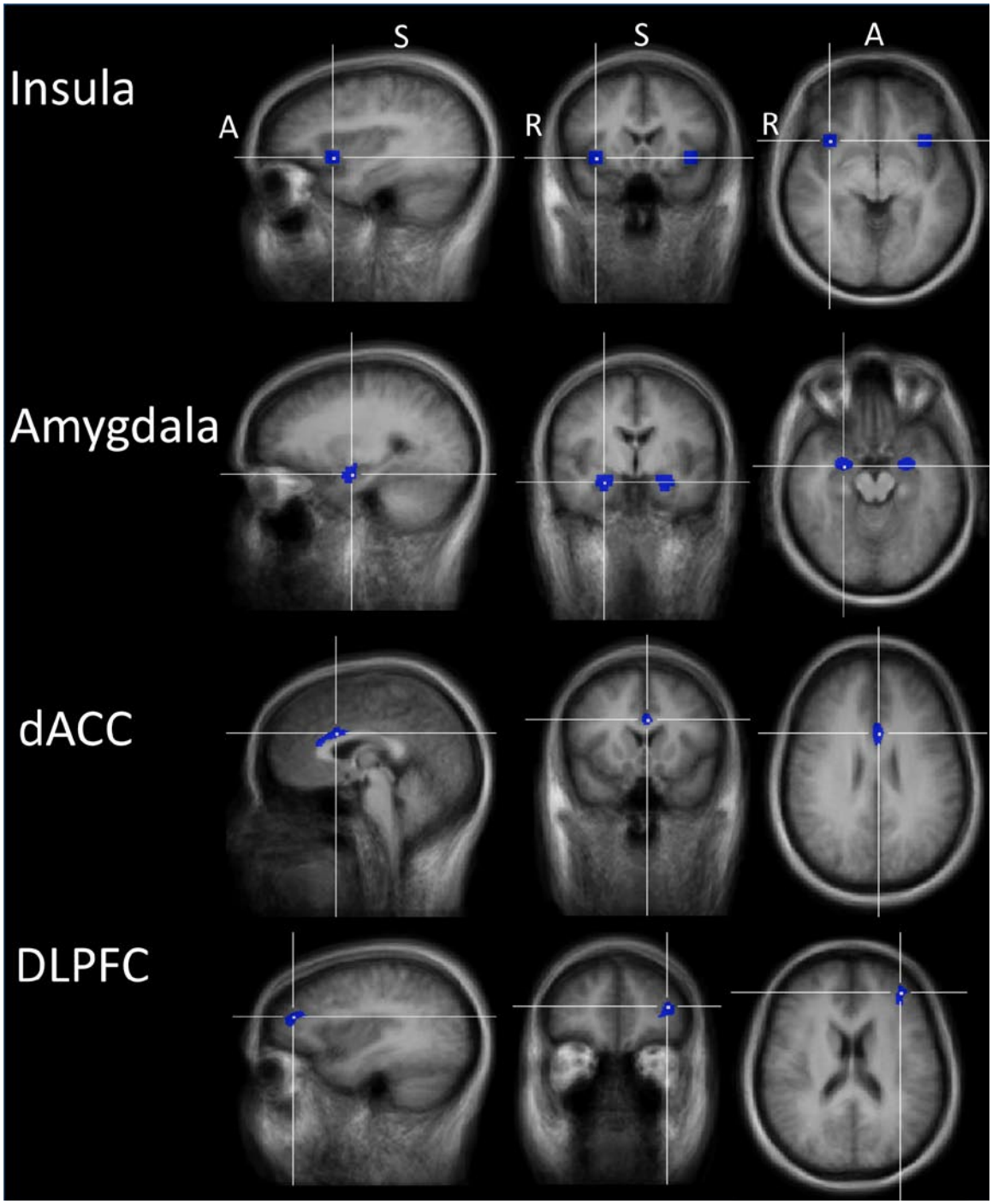

Figure S1. Regions of interest (ROIs) used for correlation analysis between brain fMRI reactivity to smoking versus neutral images and emotional Stroop interference effects. Insula and amygdala ROIs were defined anatomically and the dorsal anterior cingulate (dACC) and the left dorsolateral prefrontal cortex (DLPFC) ROIs were defined by the functional connectivity analysis. The coordinates used to anatomically define the amygdala were acquired using the AFNI atlas (analysis of functional magnetic resonance images, http://afni.nimh.nih.gov/afni/doc/misc/afni_ttatlas/). To define the insula, a cube was drawn within the anterior insula that visually corresponded with anterior insula functional activation reviewed by Craig (1). The cube was drawn in the right anterior insula and a mirror ROI was created for the left anterior insula. Insula: cross hairs located at Talairach coordinates (2) x=34, y=13, and z=5. The right and left insula each contain 1000 voxels. Amygdala: cross hairs located at x=22, y=-6, and z=-17. The right and left clusters each contain 1148 voxels. Dorsal ACC: Cross hairs located at x=-2, y=11, and z=25. This cluster contains 1098 voxels. Left DLPFC: Cross hairs located at x=-36, y=43, and z=16. This cluster contains 1131 voxels. A, anterior; S, superior; R, right.

Table S1. Whole-Brain Analysis: Slip (smoking > neutral) > Abstinence (smoking > neutral)

Brain Area, Brodmann Area, and Side refer to the location of each cluster of contiguous voxels. Talairach and Tournoux coordinates (2) refer to the center of mass for each cluster of continuous voxels. The t values refer to the maximum t statistic in each cluster. Voxels refer to the total number of voxels per cluster.

Brain Area	Brodmann Area	Side	Tal X	Tal Y	Tal Z	t	Voxels
Insula, Claustrum, Putamen	13	R	34	-6	-3	4.8	1866
Insula, Inferior Frontal Gyrus	13, 47	R	35	18	-3	4.2	453
Insula, Claustrum, Putamen	13	L	-32	-10	0	4.8	1595
Insula, Inferior Frontal Gyrus	13, 45	L	-29	28	3	4.3	284
Insula, Claustrum, Putamen	13	L	-28	3	14	3.5	103
Insula	13	L	-38	0	7	3.2	70
Cingulate							
Anterior Cingulate, Medial Frontal Gyrus	9, 32		3	40	20	3.6	173
Anterior Cingulate, Medial Frontal Gyrus	9, 32		1	45	27	3.6	247
Posterior Cingulate, Medial Frontal Gyrus	6, 23, 31		3	-29	38	5.8	1303
Frontal Cortex							
Inferior Frontal Gyrus	9, 44	R	49	11	18	5.0	2271
Middle Frontal Gyrus	10	R	44	34	15	4.6	1492
Precentral Gyrus	6	R	35	8	35	3.3	101
Middle Frontal Gyrus	9	R	31	32	37	4.3	106
Middle Frontal Gyrus	8	R	9	45	39	4.0	681
Medial Frontal Gyrus	8		2	23	47	4.1	364
Medial Frontal Gyrus	6	L	-9	-14	49	5.0	379
Precentral Gyrus	4	L	-20	-25	57	3.7	47

Precentral Gyrus	6	L	-24	-16	54	4.1	90
Inferior Frontal Gyrus	46	L	-44	34	12	3.5	132
Inferior Frontal Gyrus	44	L	-48	14	9	4.0	386
Middle Frontal Gyrus	46	L	-48	20	26	3.5	68
Parietal							
Inferior Parietal Lobule	40	R	55	-31	31	3.7	182
Postcentral Gyrus	2	R	50	-18	32	3.8	209
Inferior Parietal Lobule	40	R	42	-32	30	3.2	72
Inferior Parietal Lobule	40	R	33	-38	29	3.6	53
Precuneus	7	L	-7	-64	42	3.5	137
Inferior Parietal Lobule	40	L	-50	-40	42	4.0	155
Inferior Parietal Lobule	40	L	-57	-43	24	3.4	105
Temporal							
Angular Gyrus	39	R	58	-39	21	3.1	59
Middle Temporal Gyrus	37	R	49	-42	-5	4.8	1297
Middle Temporal Gyrus	21	R	53	-30	-5	3.6	44
Superior Temporal Gyrus	39	R	47	-58	20	3.3	38
Superior Temporal Gyrus	38	R	42	3	-13	3.5	171
Parahippocampal Gyrus	36	R	30	-34	-13	3.4	89
Parahippocampal Gyrus	36	R	18	-26	-18	3.8	849
Parahippocampal Gyrus	36	L	-23	-35	-8	3.8	136
Middle Temporal Gyrus	37	L	-52	-55	-10	4.1	964
Occipital							
Lingual Gyrus	18		-3	-72	-14	3.8	727
Fusiform Gyrus	19	L	-26	-56	-10	3.9	140
Fusiform Gyrus	19	L	-29	-72	-17	3.8	287
Fusiform Gyrus	19	L	-42	-70	-16	3.5	40
Subcortical							

Amygdala	L	-29	-9	-19	4.2	160
Thalamus, Putamen	R	19	-11	11	4.6	619
Cerebellar Vermis and Hemispheres		9	-55	-18	4.7	1915
Cerebellar Vermis		-3	-61	-20	3.5	137
Cerebellar Vermis		-9	-54	-15	3.5	258
Brainstem, Ventral Tegmental Area, Substantia Nigra		0	-12	-5	4.7	502
Brainstem	L	-11	-17	-20	3.8	93

L, left; R, right

Table S2. Functional Connectivity: Network data from all subjects

Brain Area, Brodmann Area, and Side refer to the location of each cluster of contiguous voxels. Talairach and Tournoux coordinates (2) refer to the center of mass for each cluster of continuous voxels. The t values refer to the maximum t statistic in each cluster. Voxels refer to the total number of voxels per cluster.

Brain Area	Brodmann Area	Side	Tal X	Tal Y	Tal Z	t	Voxels
Including: Superior Frontal Gyrus, Middle Frontal Gyrus, Inferior Frontal Gyrus, Superior Temporal Gyrus, Middle Temporal Gyrus, Inferior Parietal Lobule, Supramarginal Gyrus, Precuneus, Cuneus, Middle Occipital Gyrus, Lingual Gyrus, Insula, Caudate, Putamen, Thalamus, Brainstem, Amygdala, Cerebellar Hemispheres	6, 7, 9, 10, 13, 17, 18, 19, 21, 22, 37, 38, 40		3	-28	9	16.6	263552
Anterior and Posterior Cingulate, Medial Frontal Gyrus, Precuneus	6, 7, 8, 9, 10, 23, 24, 32		3	-14	39	13.2	30219
Middle Frontal Gyrus	8	R	46	-10	44	9.2	216
Precentral Gyrus	6	R	29	-10	54	10.6	520
Precentral Gyrus	4	R	25	-27	54	8.8	706
Precentral Gyrus	4	L	-31	-15	51	8.6	577
Middle Frontal Gyrus	10	R	28	49	19	9.2	254
Precentral Gyrus	6	L	-38	-7	45	8.2	53
Precuneus	7	L	-12	-49	44	8.5	57
Fusiform Gyrus	37	L	-32	-55	-19	8.4	111
Cerebellum		R	22	-38	-26	8.2	39

L, left; R, right

Table S3. Functional Connectivity: Slip subjects > Abstinence subjects

Brain Area, Brodmann Area, and Side refer to the location of each cluster of contiguous voxels. Talairach and Tournoux coordinates (2) refer to the center of mass for each cluster of continuous voxels. The t values refer to the maximum t statistic in each cluster. Voxels refer to the total number of voxels per cluster.

Brain Area	Brodmann Area	Side	Tal X	Tal Y	Tal Z	t	Voxels
Insula	13	L	-35	12	-7	-4.7	805
Insula	13	L	-31	-1	6	-3.2	41
Insula, Inferior Frontal Gyrus	13, 47	L	-42	22	-2	-3.7	48
Anterior Cingulate	24		0	19	23	-3.9	979
Posterior Cingulate	31	L	-13	-42	43	-3.3	132
Inferior Frontal Cortex	47	R	50	22	3	-4.9	301
Middle Frontal Gyrus	10	R	43	40	12	-4.0	321
Superior Frontal Gyrus	10	R	31	52	12	-3.3	64
Superior Frontal Gyrus	9	L	-14	53	26	-4.0	220
Middle Frontal Gyrus	10	L	-33	43	15	-4.3	1160
Precentral Gyrus	6	L	-37	4	23	-3.5	121
Precentral Gyrus	6	L	-56	-6	29	-3.5	128
Middle Temporal Gyrus	37	L	46	-53	-5	-4.0	816
Superior Temporal Gyrus	41	L	-44	-37	20	-3.3	67
Middle Temporal Gyrus	21	L	-57	-58	1	-3.3	32
Precuneus	7	R	9	-66	38	-3.5	213
Precuneus	31	R	2	-68	22	-3.2	52
Supramarginal Gyrus	40	R	49	-51	24	-3.3	250
Posterior Cingulate Gyrus	31	L	-13	-42	43	-3.3	132
Angular Gyrus	39	L	-49	-64	25	-4.6	1524

Postcentral Gyrus	3	L	-59	-15	24	-3.4	146
Lingual Gyrus	18	R	5	-67	-7	-3.3	106
Cuneus	18	R	1	-75	16	-3.2	42
Putamen		L	-19	3	2	-3.7	266
Putamen		L	-30	-14	5	-3.0	42
Cerebellum Hemisphere		R	11	-54	-10	-3.6	236
Cerebellum Hemisphere		R	10	-42	-13	-3.2	139
Cerebellum Hemisphere		L	-16	-56	-16	-3.8	1175

L, left; R, right

1. Craig AD (2009): How do you feel--now? The anterior insula and human awareness. *Nat Rev Neurosci*. 10:59-70.
2. Talairach J, Tournoux P (1988): *Co-Planar Stereotaxic Atlas of the Human Brain: 3-Dimensional Proportional System: An Approach to Cerebral Imaging*. New York: Thieme Medical Publishers.